

Electronic supplementary information

**Self-Reporting of Damage in Underwater Hierarchical Ionic Skins
via Cascade Reaction-Regulated Chemiluminescence**

Liangying Jia, Jing Xiao, Jiwei Cui, Jingcheng Hao, and Xu Wang*

National Engineering Research Center for Colloidal Materials & Key Laboratory of Colloid and Interface Chemistry of the Ministry of Education, School of Chemistry and Chemical Engineering, Shandong University, Jinan, Shandong 250100, P. R. China

*Corresponding author: wangxu@sdu.edu.cn

Video 1. Self-reporting of damage in underwater HI-skins

Video 2. Underwater self-healing of HI-skins

Video 3. Sensing performance of underwater HI-skins before damage and after self-healing

Experimental Section

Materials: P(VDF-HFP) was purchased from 3M Co. (3M Dyneon Fluoroelastomer FC, HFP content higher than 40%). EMITFSI, cerium (IV) sulfate ($\text{Ce}(\text{SO}_4)_2$), ST, and BPEA were obtained from Shanghai Macklin Biochemical Co., Ltd. (Shanghai, China). DNPO was acquired from Tokyo Chemical Industry Co., Ltd. (Shanghai, China). DPA was purchased from Aladdin Reagent Company (Shanghai, China). CaO_2 was obtained from Sigma-Aldrich (St. Louis, MO). All other reagents were purchased from Sinopharm Chemical Reagent Co., Ltd (Shanghai, China).

Fabrication of HI-skins: The obtained HI-skins are defined as x EMITFSI, where x is the mass ratio of EMITFSI to P(VDF-HFP). It is worth noting that the HI-skins were composed of four layers of films and the mass ratio of EMITFSI to P(VDF-HFP) was consistent in each layer. Taking 0.8 EMITFSI for example, P(VDF-HFP) (5 g) and EMITFSI (4 g) were first dissolved in acetone (35 mL) at room temperature to obtain a well-dispersed solution and then the solvent was removed by reduced pressure distillation. The obtained mixtures were dried under vacuum overnight and then compression-molded to obtain the outermost two transparent films with a thickness of 0.5 mm. The middle two layers were established according to the above-mentioned method, except that DNPO (1 g), dyes (0.015 g), and CaO_2 (1 g) were added to the well-dispersed solutions, respectively. The resultant four layers of films were assembled to establish the HI-skins.

Peeling tests: The 180° peeling tests were adopted to measure the adhesion energy between each layer of the HI-skins. The prepared film with a width of 10 mm was first fixed on a Teflon film. Then, the two layers of films needed to measure adhesion energy were attached to each other, and their free ends were clamped with a tensile clamp at a speed of 20 mm/min for the peeling test.

Measurement of H₂O₂ production: H₂O₂ production was monitored by a cerium sulfate titration method based on the reduction of Ce⁴⁺ (yellow) to Ce³⁺ (colorless) by H₂O₂. First, Ce(SO₄)₂ solutions of different concentrations (0.1, 0.3, 0.5, 0.8, and 1 mM) were prepared by dissolving Ce(SO₄)₂ in 0.5 M sulfuric acid, followed by measurements by UV-vis spectroscopy at 316 nm to establish a calibration curve. To measure time-dependent H₂O₂ production, an ionogel film (size: 13 mm × 7 mm × 0.5 mm) containing CaO₂ was placed in a centrifuge tube with 3 mL of deionized water. Then, 300 μL of aqueous solution was taken out from the centrifuge tube at fixed intervals and an equal amount of fresh deionized water was subsequently added. The obtained aqueous solution containing H₂O₂ was mixed with the 1 mM Ce(SO₄)₂ solution, and the absorption at 316 nm was measured by UV-vis spectroscopy. The concentration of H₂O₂ was calculated by the consumption of Ce(SO₄)₂.

Animals: All animal experiments were performed according to the Guidelines for the Care and Use of Laboratory Animals of National Institutes (China) and approved by the Animal Ethics Committee of Shandong University.

Characterizations: The tensile tests were performed on an INSTRON 3344 universal material testing machine with a tensile speed of 20 mm/min. The static contact angle of the sample was measured on a KPUSS DSA 100S drop shape analyzer. SEM and EDS mapping images were obtained with a Hitachi SU8010 microscope. UV-vis spectra of samples in 96-well plates were recorded using a microplate reader (Spark®, TECAN). CL intensities of samples were measured on a PerkinElmer LS-55 fluorescence spectrometer. The CL images of damaged underwater samples were observed with a bioluminescence imaging system (PerkinElmer, IVIS Spectrum, USA). The optical microscopy images were collected on an optical microscope (MP41, Guangzhou Micro-Shot Technology Co., Ltd.). FTIR spectra were recorded on a Bruker Tensor II spectrometer. Electrochemical measurements were conducted on an electrochemical workstation (CHI760E).

Statistical analysis: All data are presented as means \pm standard deviation ($n = 3$) unless otherwise stated.

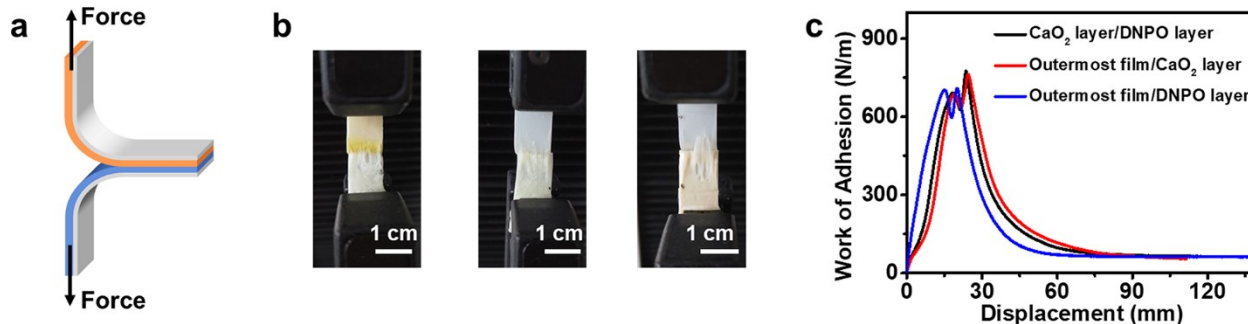


Fig. S1 (a) Schematic illustration of the 180° peeling test. (b) Photographs of the CaO₂-containing layer & DNPO-containing layer (left), the outermost transparent film & DNPO-containing layer (middle), the outermost transparent film & CaO₂-containing layer (right) in the

180° peeling tests. (c) Work of adhesion versus displacement curves between each layer of the HI-skins during the 180° peeling tests.

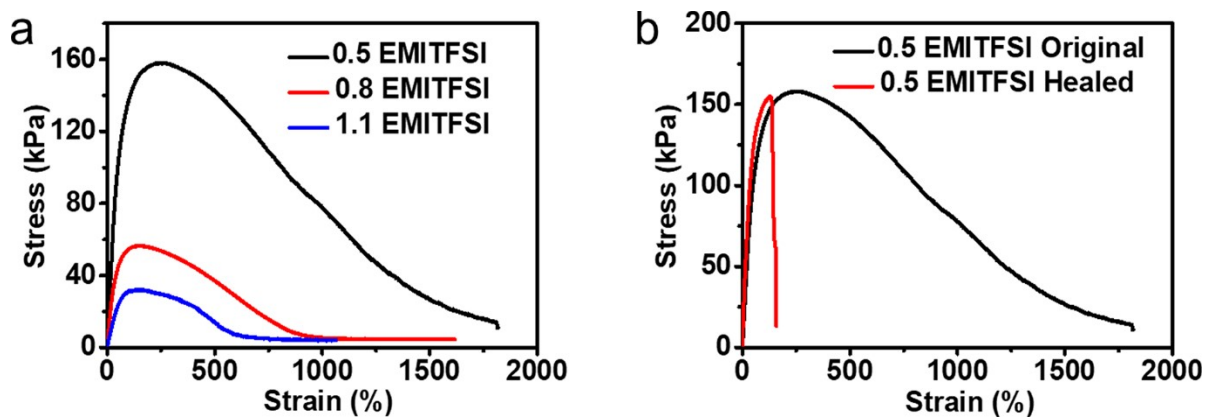


Fig. S2 (a) Stress-strain curves of HI-skins with different EMITFSI contents. (b) Stress-strain curves of 0.5 EMITFSI before damage and after damage and healing for 24 h at ambient temperature underwater.

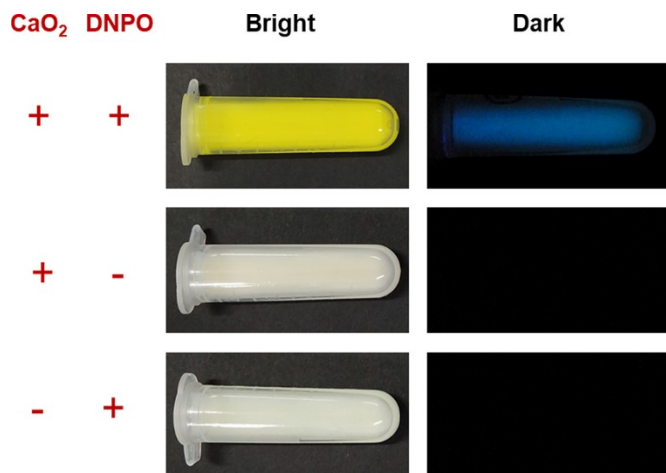


Fig. S3 Photographs of dye acetone solutions with CaO₂ and/or DNPO.

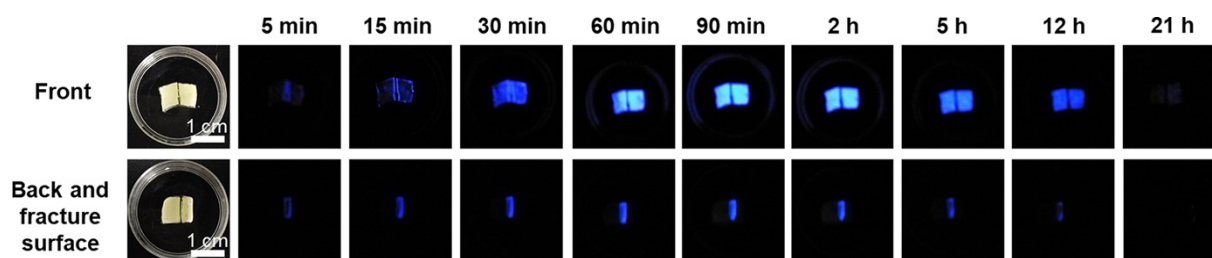


Fig. S4 Photographs showing the time-dependent CL intensities of the front (upper row) and back (lower row) of damaged underwater HI-skins.

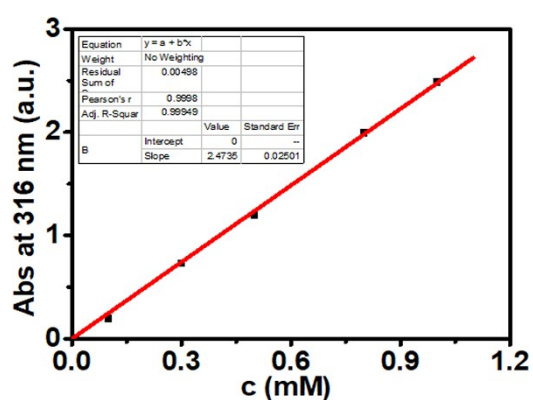


Fig. S5 Calibration curve of the absorbance of $\text{Ce}(\text{SO}_4)_2$ in 0.5 M sulfuric acid at $\lambda = 316$ nm.

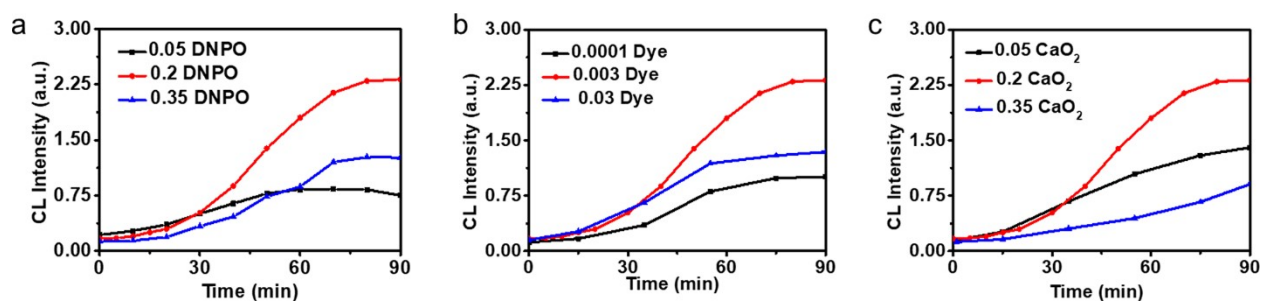


Fig. S6 Time-dependent CL intensities of damaged underwater HI-skins with different mass ratios of DNPO/P(VDF-HFP) (a), dye/P(VDF-HFP) (b), and CaO_2 /P(VDF-HFP) (c).

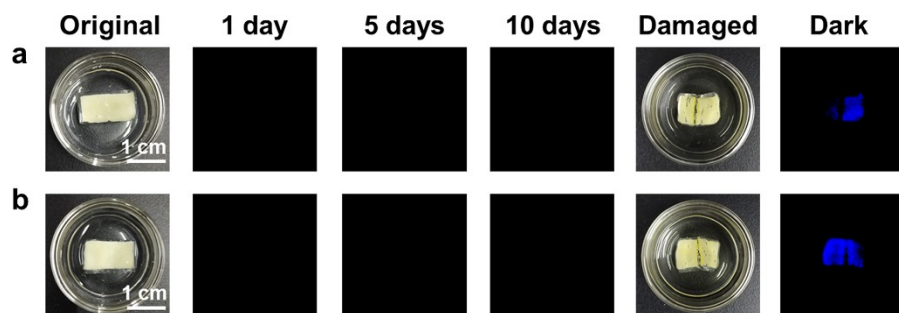


Fig. S7 Photographs showing the damage-reporting behaviors of HI-skins after being placed in water (a) and in an aqueous H_2O_2 solution with a H_2O_2 content of 2% (b) for 10 days.

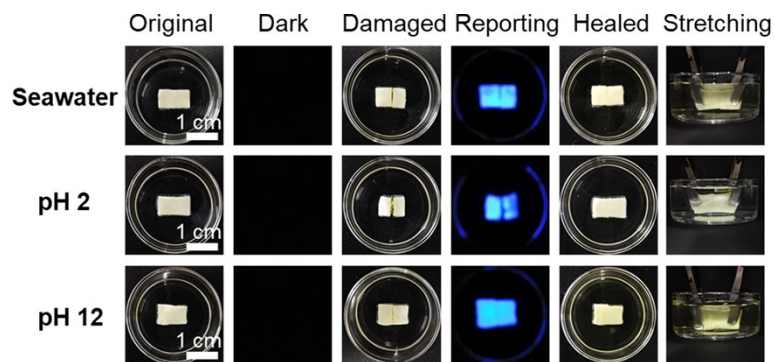


Fig. S8 Photographs showing the self-reporting behaviors of HI-skins under different conditions.

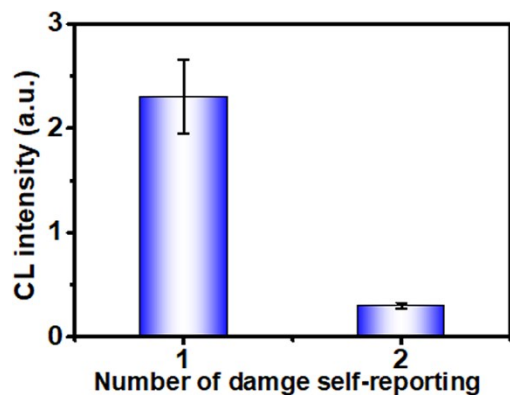


Fig. S9 Self-reporting properties of underwater HI-skins after different damage-healing cycles.

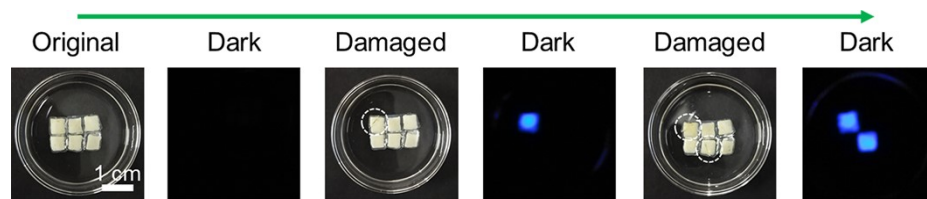


Fig. S10 Photographs showing the self-reporting behavior of a material with isolated self-reporting domains for multiple damage events. The white circles indicate the damaged domains.

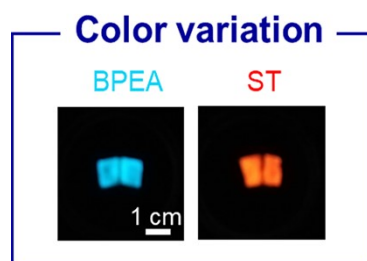


Fig. S11 Photographs of the self-reporting sides of underwater HI-skins containing different dyes.

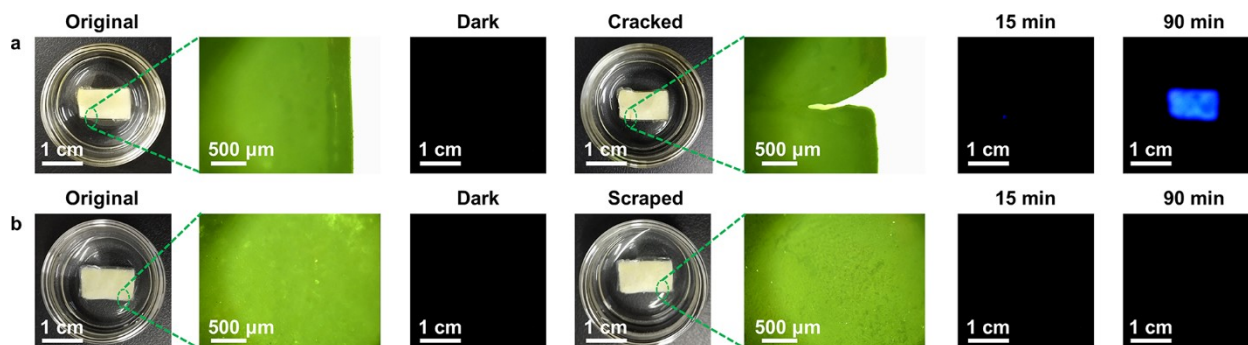


Fig. S12 Photographs and optical microscopy images of underwater HI-skins before and after crack (a) and scrape (b) for different time periods.

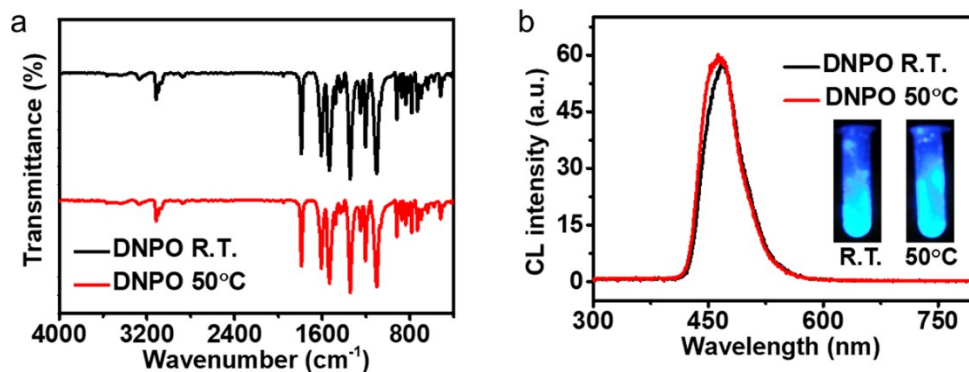


Fig. S13 (a) FTIR spectra of untreated DNPO (black curve) and DNPO after heating at 50°C for 12 h (red curve). (b) CL spectra of untreated DNPO (black curve) and DNPO after heating at 50°C for 12 h (red curve) when reacting with 30% H₂O₂ and dye for 2 min. The insets in (b) are the photographs of untreated DNPO (left) and DNPO after heating at 50°C for 12 h (right) when reacting with 30% H₂O₂ and dye for 2 min.

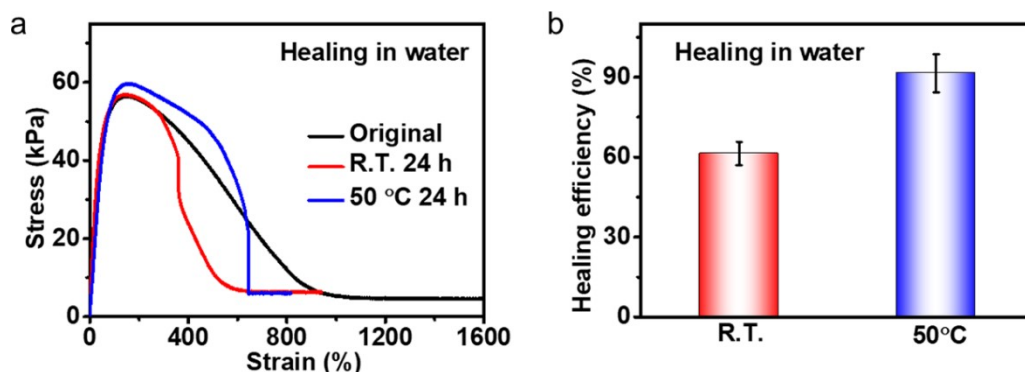


Fig. S14 (a) Stress-strain curves of HI-skins before damage and after damage and healing for 24 h at different temperatures. The strain failure point of the HI-skins healed at 50°C in water for 24 h is smaller than that healed in air, which may be due to the re-entanglement of the polymer chains at high temperature in water for a long time. Nevertheless, the toughness of the HI-skins healed at 50°C in water for 24 h could reach 90% of the original HI-skins, indicating that this healing method is effective. (b) Healing efficiency of damaged HI-skins after healing for 24 h at different temperatures.

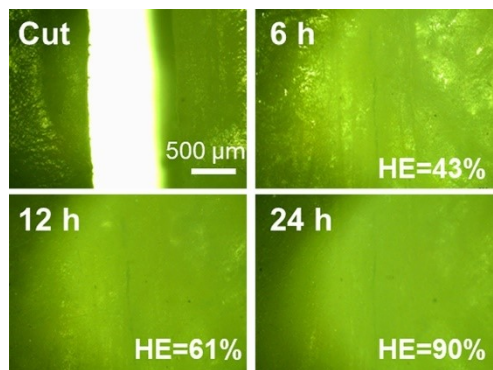


Fig. S15. Optical microscopy images of damaged HI-skins after healing for different time periods at 50°C in water. The healing efficiency (HE) obtained by tensile tests is shown in the images.

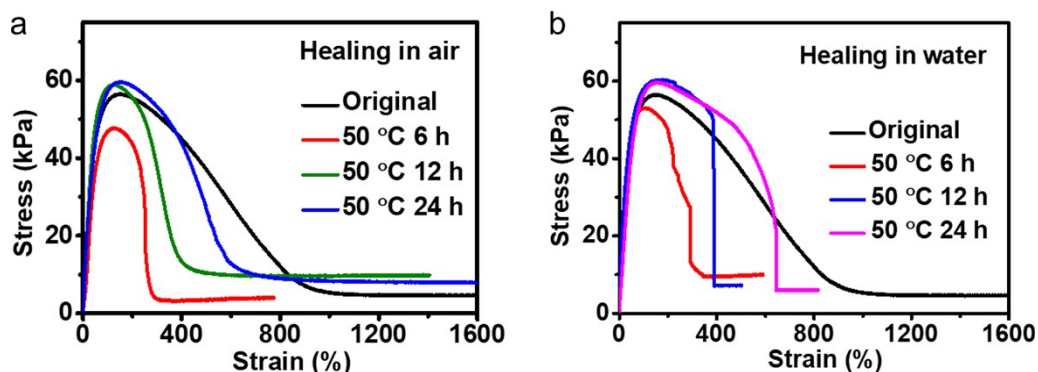


Fig. S16 Stress-strain curves of HI-skins before damage and after damage and healing for different time periods in air (a) and in water (b).

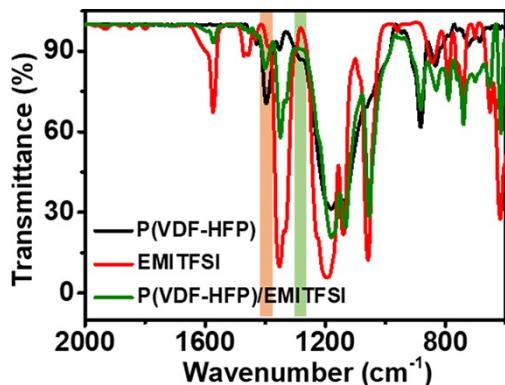


Fig. S17 FTIR spectra of P(VDF-HFP), EMITFSI, and P(VDF-HFP)/EMITFSI ionogels.

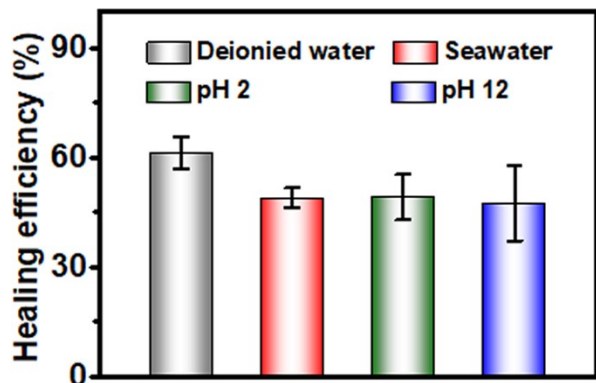


Fig. S18 Healing efficiency of damaged HI-skins after healing for 24 h at room temperature in different aquatic environments.

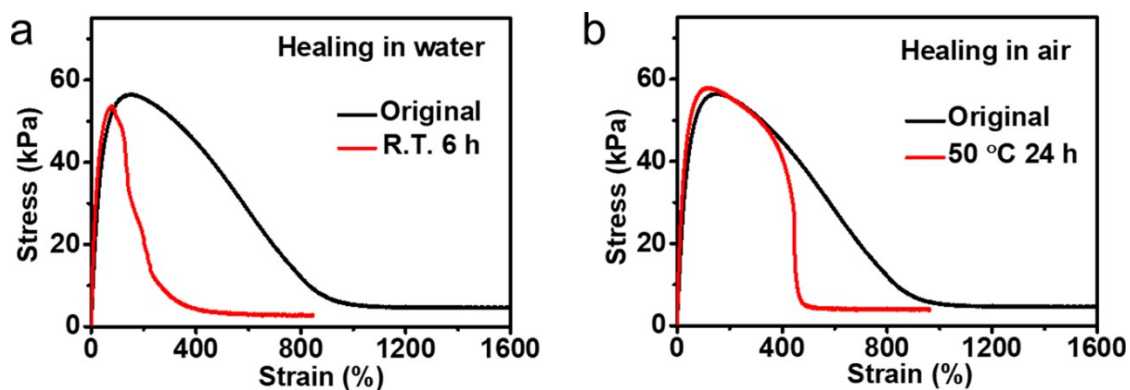


Fig. S19 Stress-strain curves of original HI-skins and healed-aged HI-skins after healing for 6 h at room temperature (a) or for 24 h at 50°C (b). The aged HI-skins were obtained by placing the freshly damaged samples in water for 1.5 h.